VISUAL ECOLOGY OF AUSTRALIAN FLATHEAD

Anthony J. Seward

A thesis submitted in partial fulfilment of the requirements for the degree of Master of Research in the Department of Biological Sciences Macquarie University Sydney, New South Wales

14/10/2018

Declaration page for the Masters of Research thesis

This thesis is written in the form of a journal article from The Journal of Vision Research

Declaration

All research described in this report is my own original work.

This work has not been submitted for a higher degree to any other university or institution.

Anthony John Seward

14/10/2018

Table of contents

Acknowledgements

I would like to give thanks to Macquarie University for providing the necessary equipment and research space. I would like to also thank the staff at the Macquarie Fauna park for help in animal care and the Macquarie Microscopy team for their training and assistance.

Thanks to both my supervisor Associate Professor Dr Nathan Hart and Dr Laura Ryan for their patience and assistance, also my lab group: Olivia, Yuri, Lou and Sian. The collective expertise and support venturing into this new field of research made this possible.

I would also like to thank my family, in particular my partner Kataya, without whom this would not have been possible.

Abstract

Despite our growing understanding of fish visual ecology, the visual systems of relatively few benthic marine species have been described in detail. Flatfish are one of the largest groups of benthic fish, and in the New South Wales (NSW) region of the East coast of Australia, the *Platycephalidae* (flatheads) are the predominant and most diverse flatfish family. Flatheads are also important economically, accounting for $2.1 million in NSW fisheries revenue annually. The aim of this study was to investigate the anatomy and spectral sensitivity of the eyes of flatheads to identify correlations with habitat and behaviour, using one or more of the species found in NSW waters. Microspectrophotometry (MSP) was used to measure the spectral absorbance properties of the visual pigments in the rod and cone photoreceptors of the dusky flathead (*Platycephalus fuscus*) and blue-spotted flathead (*Platycephalus caeruleopuntatus*). The MSP data show that *P. fuscus,* which predominantly occupies shallow estuarine habitats, possesses multiple cone visual pigments with peak sensitivities in the short ('blue') to medium ('green') wavelength range of the spectrum. MSP data of *P. caeruleopuntatus,* which predominantly occupy deeper water marine habitats, shows that they possess similar multiple cone visual pigments to *P. fuscus,* but with a noticeable shorter wavelength shift in the single cone visual pigment. Spectrophotometry of the ocular media of both species reveals that the spectral absorbance of the lens limits the transmission of short wavelength light to the retina and effectively blocks wavelengths below about 400 nm. The topographic distribution of retinal neurons was also measured to establish the areas of the visual field sampled with high resolution. *P. fuscus* and *P. caeruleopuntatus* display a similar distributional topography with an elongated area present in the dorsal retina. The results of this study are compared with findings for other benthic fish species.

Introduction

In most vertebrates, vision is a crucial sensory system and adaptations in the structure and function of the eye often reflect various aspects of a species' life history and ecology. The study of the relationship between eye 'design' and habitat or behaviour is known as visual ecology.

Vertebrates typically possess a single-chambered camera-like eye. Light enters the eye through the cornea and pupil and is focused by a lens onto a mosaic of photoreceptors in the retina (Walls, 1942; Land & Nilsson, 2012). Light is transduced into a neural signal by the photoreceptors, which is further modulated and processed by bipolar, horizontal and amacrine cells, before being sent to the higher visual centres in the brain via the axons of ganglion cells, which form the optic nerve (Walls, 1942; Land & Nilsson, 2012).

Two of the primary forms of information gathered by the eye are i) the spectral composition of the light reflected from or transmitted by an object and ii) the spatial arrangement of objects relative to others. Both forms of information are crucial in governing the behavioural responses of the animal, and both are affected by the physiology and the anatomical structure of the retina (Land & Nilsson, 2012).

The range of the wavelengths to which an animal is sensitive is determined largely by the types of visual cone pigments present in the retinal photoreceptors (Walls, 1942). Two main types of photoreceptors can be found in the retinal mosaic: rods and cones. Rods are typically responsible for vision in low light (scotopic) conditions and have little or no role in colour discrimination (Partridge *et al.*, 1988). Cones, on the other hand, are responsible for colour vision (where multiple chromatic types are present) and vision in bright light (photopic) conditions. The diversity, abundance and organisation of photoreceptors in the retinal mosaic determine light capturing capabilities, spectral sensitivity and resolving power of the eye under differing light conditions (Lythgoe, 1968; Lythgoe & Partridge, 1989).

In the ocean, many different light environments have been identified and categorised (Jerlov, 1968; Lythgoe, 1968; McFarland & Loew, 1983). The differences in light environments are driven by the optical properties of natural waters, which scatter and absorb light to a much higher degree than air so that the amount and spectral distribution of light in water changes rapidly with depth. Other factors such as turbidity, dissolved organic matter and suspended particulates can also alter light scattering and absorption in the water column

(Lythgoe, 1968). Coastal environments have higher concentrations of organic particulate matter and therefore tend to have a greenish tint (McFarland, 1991). In clear water, maximum transmission spectrum is about 460nm and falls off at shorter and longer wavelengths; therefore, species living at depth tend to have blue sensitive photoreceptors (Lythgoe & Partridge, 1989; McFarland, 1991).

In the aquatic environment, many eye structures have converged upon similar designs (Walls, 1942; Land & Nilsson, 2012; Marshall, 2017), optimised for light detection in the aquatic medium. For example, most fishes possess a large fixed corneal aperture and a large spherical crystalline lens with a refractive index similar to that of water, which improves light refraction and focussing, in the aquatic environment (Walls, 1942; Land & Nilsson, 2012). The retina, on the other hand, experiences a great deal of variation between aquatic vertebrates.

Retinal structures in teleost species vary not only between species but even within species (Shand *et al.*, 2002). The retinal mosaic in teleosts, unlike other vertebrates, continuously grows over the animal's lifetime (Collin & Pettigrew, 1989), changes during development and displays high variability between species. The rod: cone ratio in the retina is a balance that determines light capture capabilities under differing light conditions. Morphological adaptions such as corneal filtering can increase capture efficiency by reducing noise on the retina. Other adaptations like reflective structures tapetum (Ollivier *et al.*, 2004) can increase light capture by directing more light onto the photoreceptors, allowing for more wavelength spectra sensitivity without sacrificing overall sensitivity.

The sensitivity of the eye to specific wavelength spectra is dependent on the diversity of visual pigments found in the cone photoreceptors. The variability of visual pigments in teleosts has been correlated with changes in the spectral distribution of light in aquatic environments (Lythgoe *et al.*, 1994; Marshall *et al.*, 2003). The variability in visual pigments of photoreceptors is often the result of a functional trade-off, between light capture and colour discrimination. Possessing a high diversity and abundance of cone types can increase colour discrimination and vision in the well-lit upper aquatic zones, but doing so would reduce the abundance of rods, decreasing visual capabilities in the dim light aquatic regions.

Photoreceptors are responsible for light sensitivity, but the link between the photoreceptors and the brain lies in the distribution and organisation of the ganglion cells in the retina (Lythgoe

& Partridge, 1989). The spatial distribution of ganglion cells in the retina determines the absolute maximal spatial resolving power of the animal (Collin & Pettigrew, 1989).

The organisation of ganglion cells in the retina according to 'Terrain theory' of Hughes (1977) follows two predominant topographical distribution patterns in vertebrate retina, either a concentrated area centralis or a horizontal streak, both have been correlated with morphological and behavioural adaptations (Collin & Pettigrew, 1988b, 1988a). An area centralis is a concentric area of high neuronal density towards the pole of the retina and is associated with high visual resolution in a specific area of the visual field and is often correlated with distinctive eye mobility (Collin & Pettigrew, 1988a). A horizontal streak pattern of neuronal cell distribution is instead thought to provide a panoramic view of the visual horizon at higher spatial resolution without the need of extensive eye movements, which might give away the position of an otherwise camouflaged animal (Collin & Pettigrew, 1988a; Litherland & Collin, 2008).

Morphological adaptions in benthic teleosts are often observed, such as a dorso-ventrally flattened physiology and turreted eyes (Savino & Stein, 1989; Marshall *et al.*, 2015), that presumably aid in allowing such animals to position themselves on the benthos and remain camouflaged, yet observe a wide field of view, laterally and upwards into the water column. Some teleost species have even gone so far as to bury themselves in the benthos to aid further in camouflaging them as they wait to ambush prey that passes above (Douglas & Lanzing, 1981; Schieber *et al.*, 2012; Nelson *et al.*, 2016). In this scenario, a predator is using the visual contrast generated by the downwelling light that illuminates their potential prey from above and this may be reflected in their retinal topography (Loew & Lythgoe, 1978; Litherland & Collin, 2008; Marshall *et al.*, 2015). Both area centralis (e.g. sandlance *Limnichthyes fasciatus*) and horizontal streak (e.g. European hake *Merluccius merluccius*) retinal topographic types have been observed in benthic ambush predators (Bozzano & Catalán, 2002; Collin & Collin, 1988).

Marine teleosts visual systems, whilst not neglected, have not been studied as extensively as that of freshwater teleosts (Marshall, 2017). For the marine teleosts visual systems that have been examined, those studies have focused on the adaptations derived in unique environments, pelagic species in coral reefs (Collin & Pettigrew, 1988a) and deep sea species (Partridge *et al.*, 1988; Partridge *et al.*, 1989), with only a cursory glance at benthic species in those environments. The largest group of marine benthic teleosts are classified as flatfish, forming

one of the most abundant taxonomic groups in the northern hemisphere (Pauly, 1994; Pauly *et al.*, 1998). Flatfish are highly diverse in morphology and behaviour. Some species, such as the Atlantic halibut (*Hippoglossus hippoglossus*), grow up to 4.7m (Geffen, *et al.*,, 2007; Hopper, 2013) and are found across all environmental niches, from estuarine coastal regions (Amezcua & Nash, 2001) to deep-sea (>1200m) (Sohn, 2009; Duffy-Anderson *et al.*, 2013). In the northern hemisphere, the most abundant flatfish are halibut (*Pleuronectidae*) and flounder (*Bothidae*) (Pauly, 1994). Halibut and flounder are of interest in some regions as they are some of the most abundant taxa , but also morphologically due to the visual metamorphosis, they undergo with optical migration (Geffen *et al.*, 2007). Optical migration occurs before settlement, after the larval life history stage in which one eye migrates to the other side of the head, either through or around front of the head, but this process is still in need of further study. For those reasons the visual systems of these teleost families have been the focus of several studies over the years (Hoke *et al.*, 2006; Iwanicki, 2016) and have revealed some highly diverse variations between species that still require further exploration (Bozzano & Catalán, 2002).

In the Indo-pacific region, the flathead (*Platycephalidae*) are the most abundant and diverse family of flatfish and are of importance to both recreational and commercial fisheries (Barnes *et al.*, 2011). The general and visual ecology of this family has remained largely unexplored, scientifically (Barnes *et al.*, 2011; Hunt *et al.*, 2015). Flathead share many behavioural similarities with halibut and flounder but are morphologically divergent in many ways, for example, they do not undergo optical migration, and some species have dorsally extended or turreted eyes (Gray & Barnes, 2008; Bray, 2017). Some investigations into the selective pressures that have led to the development of such visual and morphological adaptations in the visual apparatus of benthic fishes have been undertaken, but for a better understanding of this variation further study is required.

Given their morphological and ecological diversity, the *Platycephalidae* are potentially an ideal taxon in which to study the variability of visual systems between closely related species (Froese & Pauly, 2010; Bray, 2017). Dusky flathead (*Platycephalus fuscus*) are the largest species of flathead in Australian waters (Bray, 2017). They inhabit both brackish estuarine and shallow marine habitats, feeding on a diverse range of crustaceans, invertebrates and small teleosts (Barnes *et al.*, 2011). Dusky flatheads are highly abundant and of interest to both fisheries and recreational fishermen, the estimated annual catch rate for NSW Australia is in

excess 400 tonnes per annum (Gray & Barnes, 2015). The blue-spotted flathead (*Platycephalus caeruleopunctatus*) occupies similar shallow marine habitats to the dusky flathead but also inhabit deeper-water marine habitats (Bray, 2017), feeding on a similar diversity of prey. Knowledge of the visual systems of both these species apart from a note of corneal iridescence in dusky flatheads (Ullmann *et al.*, 2012) is non-existent. The diverse environmental and ecological niches these two species cover, exposes them to a range of differing aquatic light conditions. The study of the visual capabilities of two closely related benthic species will provide information on behavioural and environmental pressures that shape the visual ecology of benthic vertebrates.

The aim of this study was to examine the visual specialisations of both dusky and blue-spotted flathead in relation to their environmental niche. The topographic distribution of neurons across the retina was measured to identify any areas of increased spatial resolution and to estimate their maximum theoretical spatial resolving power. Their spectral sensitivity was also investigated by measuring the spectral absorption properties of the visual pigments contained within their retinal photoreceptors using microspectrophotometry (MSP). The ocular media of both species was also measured using transmission spectrophotometry to determine if there is any spectral filtering of the light incident on the retina. Dusky and blue-spotted flathead were expected to have similar overall visual system structural morphology, with ganglion cell density reflective of predators that hunt from below (Litherland & Collin 2008). Variability between the species was expected to be distinct in relation to visual cone pigments. Visual cone pigments in both flathead species is expected to be more reflective of their differences in habitat, depth ranges and behaviour.

Methodology

Animals

Six dusky flathead (*Platycephalus fuscus*; 26-28 cm SL, one late-stage juvenile and five adults) and seven blue-spotted flathead (*Platycephalus caeruleopunctatus*; 22-33 cm SL, one late-stage juvenile and six adults, see Image 1.) were caught by rod and line in the greater Sydney region and at Port Stephens, New South Wales (NSW), Australia, under permit from the NSW Department of Primary Industries (P17/0055-1.0). Animals were dark adapted for 1-2 hours and euthanised in the dark by approved humane methods (overdose of tricaine methane-sulfonate, MS-222, 1:2000; buffered with an equal mass of sodium bicarbonate). All procedures were approved by the Macquarie University Animal Ethics Committee (ARA 2017/039).

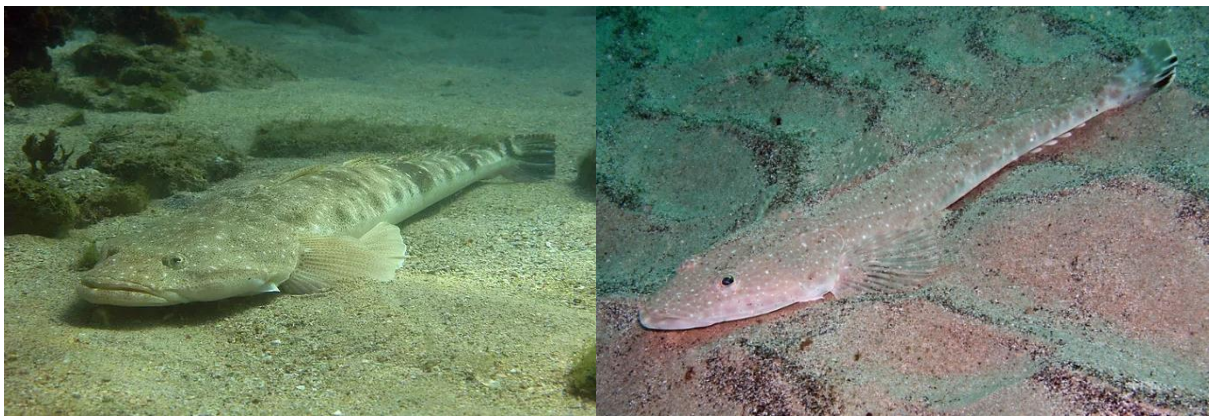

Figure 1. Photographs of Platycephalidae species; dusky flathead (*Platycephalus fuscus*) (Left) and blue-spotted flathead (*Platycephalus caeruleopunctatus*) (Right).

Removal of the eyes was conducted under dim red light. Prior to removal from the head, the orientation of each eye was marked by making a shallow burn on the dorsal aspect of the cornea and/or sclera using a surgical cautery pen. Eyes were then removed, and their axial length and equatorial diameter measured using a digital Vernier calliper.

Microspectrophotometry of retinal photoreceptors

All specimens utilised for this procedure were first dark adapted for one hour prior to the removal of the eyes. The right eye was dissected in the dark with the aid of a low-power stereomicroscope, adapted with an infrared image converter attached to one ocular, and using the illumination provided by a bank of infrared light emitting diodes. Small pieces of retina

(approximately 1mm^2) were mounted in a single drop of 420 mosmol kg^{-1} phosphate buffered saline (PBS; pH 7.3) containing 10% dextran on a 22mm × 60mm no. 1 coverslip. The retinal tissue was teased apart using forceps, or macerated using fine scissors, and covered with a 22mm × 22mm no. 0 coverslip. Gentle pressure was applied to the top coverslip to express excess fluid and the edges of the top coverslip sealed with clear nail varnish to prevent dehydration of the preparation and movement of the top coverslip. Preparations were then stored in the fridge in a light-tight container at 4°C until use.

A single beam wavelength-scanning microspectrophotometer was used to measure the transverse spectral absorbance (330-800 nm) of individual photoreceptor outer segments to 1 nm intervals (Hart, 2004; Hart *et al.*, 2011). A prebleach spectral absorbance measurement consisted of an initial sample scan made with the beam aligned in the outer segment, and then a subsequent baseline scan made with the beam positioned in an adjacent cell-free area of the preparation. The outer segment was then bleached with full spectrum white light for two minutes and a post-bleach absorbance spectrum obtained through new sample and baseline scans.

Analysis of visual pigment absorption spectra

Absorbance spectra (*P. fuscus;* rod: 81, cone: 124 and twin cone: 129, *P. caeruleopunctatus;* rod: 99, cone: 108 and twin cone: 124) were analysed as described elsewhere (Hart *et al*, 1998). Briefly, sample and baseline scans were converted to absorbance at each wavelength. Spectra were then smoothed with a variable-point unweighted running average and normalized to the maximum and the minimum absorbance, the latter obtained by averaging the absorbance values between 680-780nm. A regression line was fitted to the absorbance data between 80% and 20% normalized absorbance on the long-wavelength limb of the spectrum and used to estimate the wavelength of maximum absorbance (λ_{max}) following the methods of (MacNichol, 1986). Spectra meeting established selection criteria were retained for further analysis (Levine & MacNichol, 1985). For display, visual pigment templates of the appropriate λ_{max} (Govardovskii *et al.*, 2000) were overlaid on the mean prebleach and difference spectra.

Histology

The left eye was hemisected and—using the burn mark made before removing the eye from the head—a small cut was made in the dorsal rim of the eyecup to preserve the orientation

of the eye. The eyecup containing the retina was then fixed in 4% paraformaldehyde in 0.1M sodium phosphate buffer (PFA, pH 7.4) and stored at 4°C, the anterior segment and lens were retained for spectrophotometry of the ocular media (see below). The diameter of the lens along the optical axis was measured using a digital Vernier calliper.

Following fixation (minimum one week), the eyecup was rinsed in 0.1M PBS and prepared for dissection. The orientation of the retina was maintained using the dorsal cut in the rim of the eyecup and other landmarks, such as the optic nerve head and falciform process. Using fine scissors, the sclera and choroid were cut away from the retina. Most of the retinal pigmented epithelium was removed using a fine paintbrush, but residual pigment was bleached by incubating the retina in a solution of 5% hydrogen peroxide in 0.1M PBS at 60˚C for 5-20 minutes.

Once bleached, the retina was rinsed in 0.1M PB (pH 7.2). The retina was then floated onto filter paper, and under a dissection microscope the vitreous humour was removed using fine scissors. Once the vitreous was removed, relieving cuts were made in the edge of the retina to allow it to lie flat. The retina was then gently moved onto a gelatinised 76 mm × 51 mm × 1 mm clear white glass slide and excess PB removed. The retina was fixed to the slide by exposure to paraformaldehyde vapour in a closed glass chamber at 65˚C for 1 hour. The retina was dried slowly over a period of 2 days in a moist chamber. Mounted retinae were then stained with Cresyl Violet 0.05% solution (pH 4.3, 18-20 minutes) using a staining protocol modified from (Ullmann *et al.*, 2012). Due to increased shrinkage, wrinkling and micro-tearing present in retinal tissue subject to the published protocol, the original xylene defatting steps were removed, and an additional rehydration step of 30% ethanol was added to prevent rehydration shock and wrinkling or detachment of the retina from the slide. Additional time was added to each step to allow for more gradual rehydration and dehydration at each step (for details see Appendix i). Once dehydrated and processed through xylene the retina was then sealed by flooding the retina with Entellan® New and covered with a 50 mm × 32 mm coverslip.

The whole-mounted retina was then analysed using an Olympus BX63 microscope fitted with a motorised stage and Olympus DP80 camera controlled by Cell Sens Entry software (Olympus, version: 1.17, core version: X V 3.16 (build 16030)).

First, a composite image of the entire retina was made using a low power (×4 / 0.16 numerical aperture NA) objective; this image served as a reference for the counting grid and

was also used to trace the outline of the retina during analysis (see below). Next, prominent retinal landmarks were viewed using a higher magnification objective (×100 / 1.40 (oil) NA) and the stage micrometer setting recorded for each landmark to calibrate the composite image outline with the coordinates used for counting.

The retina was counted using stereological principles outlined elsewhere (Coimbra *et al.*, 2009; Garza-Gisholt *et al.*, 2015). Briefly, a counting grid was applied randomly to the retinal area and counts made within a sub-region. Counts for the dusky flathead retina were made with the use of a 300 × 300 µm grid due to the smaller retinal size, and a 500 × 500 µm grid was used for the larger blue-spotted flathead retina. The counting frame for both species was 100 × 100 µm.

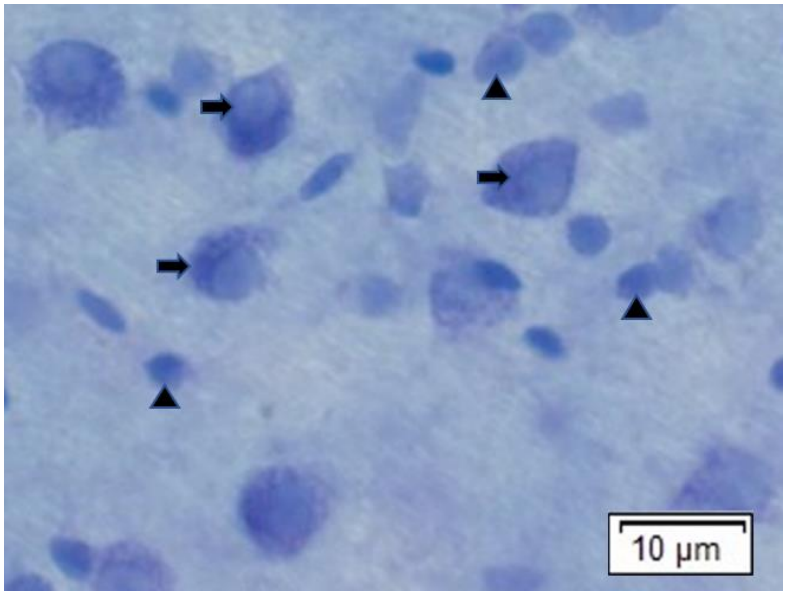

Figure 2. Photomicrograph of Nissl-stained cells in the retinal ganglion cell layer of the dusky flathead *P. fuscus*. Ganglion cells are characterised by their large polygonal cell bodies, darkly staining abundant cytoplasm and pale staining nucleus (arrows). Displaced amacrine cells in the ganglion cell layer (arrowheads) are usually round, oval or teardrop shaped and much smaller than the ganglion cells. Glial cells are darkly stained and characterised by their cylindrical or abnormal shape.

Counts of Cresyl Violet-stained cells in the ganglion cell layer were made using a x100/1.40 (oil) NA objective. Ganglion cells could be distinguished in most retinal regions by their larger sized, polygonal shaped cell bodies with Nissl staining clumped around a paler stained nucleus. However, due to difficulties in distinguishing displaced amacrine cells from

ganglion cells across the whole retina—especially in areas of high cell density— all cell bodies present in the ganglion cell layer that stained for Nissl substance were counted, except for very darkly stained glial cells (Bozzano & Catalán, 2002; Hart, 2002). This counting protocol resulted in 1101 and 566 counts from the dusky and blue-spotted flathead retina, respectively. Unfortunately, due to the restricted availability of specimens and the loss of some retinas due to earlier whole mounting attempts, good count data were only obtained from one retina for each species.

To display the topographic distribution of the neurons in the GCL of the flathead retinas, the flat-mounted retinal outline was first reconstructed into a hemisphere *in silico* using the R package 'retistruct' (Sterratt *et al.*, 2013). This procedure 'stitches' the retina back together at the cuts made in the retina to lie it flat and generates an azimuthal equidistance projection of the intact curved retina in the eyecup. First, an outline of the retina was traced (from the composite retinal image obtained prior to counting) using the polygon tool in Image J (Abràmoff *et al.*, 2004) and saved as a Region of Interest (ROI) file. The falciform process/optic nerve head was also traced in ImageJ and saved as an x-y co-ordinate text file. The pixel locations corresponding to the counting frame locations were also calculated from the outline image using the microscope stage micrometre coordinates of the identified retinal landmarks. The locations of cuts in the retinal periphery and the orientation of the retina were marked up in retistruct and the retina reconstructed.

The neuronal count data were then projected onto this reconstructed outline using the R package 'retina' (Cohn *et al.*, 2015). This package generates the spherical coordinates of the count locations in relation to the reconstructed outline, applies thin plate spline smoothing (set to 0.0005) and plots the data with appropriate contours.

Estimating visual resolution

The theoretical visual resolution maxima for both species was estimated from peak neuronal density counts of the whole-mounted retinas. The focal length (*f)* of the eye was estimated by using the axial length *l* of the lens (measured using digital callipers) using Matthiessen's ratio (1880):

$$f = 2.55(l/2) \quad (1)$$

The distance subtended by 1˚ on the retina *d* was calculated from the focal length f, using equation 2:

$$d = (2\pi f)/360 \quad (2)$$

Assuming a hexagonal distribution of ganglion cells (Theiss *et al.*, 2007; Garza-Gisholt *et al.*, 2015), the average cell-to-cell spacing *S* was calculated by using equation 3, where *D* is the peak density of ganglion cells per mm² in the extended area of the whole-mounting spatial topography counts:

$$S^2 = 2/(D\sqrt{3}) \quad (3)$$

The maximum spatial frequency *v* was then determined by using equation 4 and the calculated *S* value:

$$v = 1/(S\sqrt{3}) \quad (4)$$

The spatial resolution in cycles per degree was then determined by multiplying the value of *v* by *d* (Hart, 2002; Theiss *et al.*, 2007; Garza-Gisholt *et al.*, 2015).

Spectrophotometry of ocular media

The anterior segment and the lens from each eye were stored in 420 mosmol kg^{-1} phosphate buffered saline (PBS, pH 7.3) at 4°C prior to measurement (approximately 30 minutes). Spectral transmittance measurements (300–800 nm) of the cornea and lens along the optical axis were made in air using an Ocean Optics USB4000 spectrophotometer. Light from a 150W xenon arc lamp was delivered to the sample via a 600 µm diameter quartz fibre optic cable fitted with a quartz collimating lens (Ocean Optics). Light passing through the ocular media was collected with another quartz fibre optic cable (100 µm diameter) fitted with a cosine collector attachment (CC-3-UV, Ocean Optics) and passed to the spectrophotometer. Each spectral transmittance measurement was the average of 20 individual wavelength scans by the USB4000, and at least two separate measurements of each piece of the ocular media were measured and averaged from two specimens of each species. The mean spectra for each sample were interpolated to 1 nm intervals and normalised. The normalised measurements were used to generate a mean spectral transmittance curve of the lens and cornea (and also their arithmetic combination) for each species.

Results

General observations

The eyes of both species of flathead are located on the dorso-lateral aspect of the head and face outwards. The pupil has an irregular ovoid shape and is partially obscured by dorsal protrusion of the iris. There was a noticeable difference in the relative size of the eye (axial length) with that of the blue-spotted flathead being much larger relative to standard body length (SL) (mean ratio = 0.352) than the dusky flathead (mean ratio =0.285), despite the dusky flathead being the larger of the two species. The blue-spotted flathead also possessed a much larger choroid gland. Examination under differing light conditions revealed a corneal iridescence was present in blue-spotted flathead (Figure 3.), but was absent from any dusky flathead specimen's, contradictory to previous observations (micrograph Figure 1h. Ullmann *et al.*, 2012). A retinal tapetum was not observed in either species; however, a silvery iridescent stratum argenteum located between the choroid and the sclera (Ollivier *et al.*, 2004) was present in blue-spotted flathead.

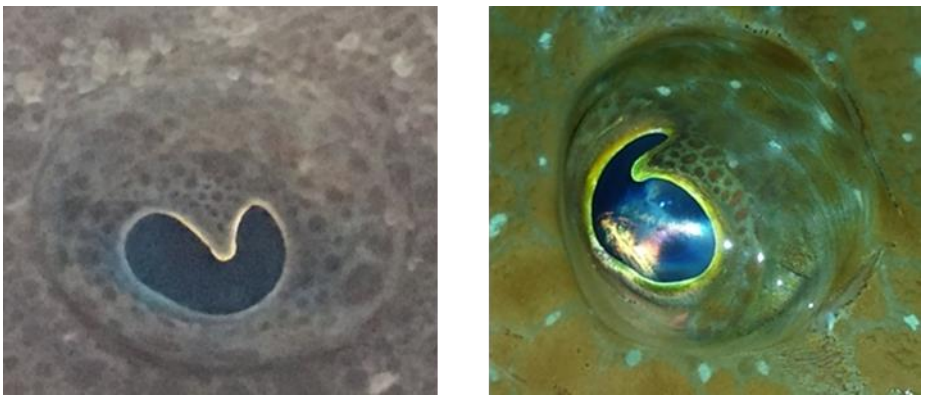

Figure 3. Dusky flathead (*P. fuscus*) eye (Left) and blue-spotted flathead (*P. caeruleopuntatus*) eye (Right).

Microspectrophotometry

Microspectrophotometric data for the dusky flatheads studied is summarised in Table 1 and Figure 4. below. The microspectrophotometric data for the blue-spotted flathead is likewise summarised in Table 2 and Figure 5. below. All visual pigment absorbance spectra from both species were considered to be rhodopsin A_1-based visual pigments, based upon goodness-of-fit to mathematical templates (Govardovskii *et al.*, 2000).

Initially, the two members of the twin cone pair were analysed separately with separate means calculated for the members having either the lower (shorter wavelength) or higher (longer wavelength) measured wavelength of maximum absorbance (λ_{max}) in the pair. However, there was little separation in the mean λ_{max} values calculated in this way and so the data were also presented as a single mean of all twin cone outer segments. The retina of the dusky flathead contained a single type of rod; its visual pigment had a mean λ_{max} at 504 nm. The dusky flathead retina contained a single cone visual pigment and twin cone visual pigments. The single cone outer segments visual pigments have a mean λ_{max} of 483 nm, and the twin cone outer segment visual pigments have a mean λ_{max} of 528 nm. (When the twin cone visual pigments were classified based on the distinction of higher and lower λ_{max} within their twin pairing, higher twin cones had a mean λ_{max} of 530 nm, and the lower twin cones had a mean λ_{max} of 526 nm.) Some visual pigment spectra with atypical λ_{max} values were measured from a few cone outer segments in both species but, because of their rarity, were not included in the analysis. These included both twin cones (blue-spotted flathead n = 2 cells; λ_{max} ~460 nm; dusky flathead n = 2 cells, λ_{max} ~470 nm) some short-wavelength sensitive single cones (dusky flathead n = 1 cell, λ_{max} ~450 nm). Further investigation is required to determine if these rare cells represent distinct photoreceptor types.

The retina of blue-spotted flathead was morphologically similar to dusky flathead in that it possessed rods, single cones and twin cones. The outer segment λ_{max} value of the rods (mean λ_{max} 508 nm) in blue-spotted flathead corresponded with the wavelengths observed in dusky flatheads. The value of the single cone outer segment visual pigments found in blue-spotted flathead was at a shorter wavelength (mean λ_{max} 461 nm) than that of the corresponding single cone in dusky flathead. The twin cones outer segment mean λ_{max} of 526 nm corresponded closely with the mean λ_{max} observed in dusky flathead. Analysis of the twin cones in blue-spotted flathead, in which twin cones were similarly classed according to higher and lower absorbance within their twin pairing, the higher twin cone (mean λ_{max} 527 nm) and lower twin cone (mean λ_{max} 525 nm), were both at close but shorter wavelengths than the corresponding twin cone visual pigments in dusky flatheads.

	Rod	Single cones	Twin cones		
			Higher	Lower	All
λ_{max} of mean prebleach spectrum (nm)	503.7	483	529.6	526.4	528
Mean prebleach λ_{max} (nm)	504.8 ±3.3	483 ±3.9	530.2 ±6.9	526.6 ±7.0	528.5 ±7.1
Number of cells	45	32	50	49	99
$\underline{\lambda}_{max}$ of mean difference spectrum (nm)	507.9	483.9	530.2	528	529.1
Absorbance change at λ_{max} of difference spectrum	0.015	0.028	0.039	0.043	0.041
Mean difference spectrum λ_{max} (nm)	509.3 ±5.0	483.2 ±5.0	530.9 ±5.7	528.4 ±5.8	529.6 ±5.9
Number of cells	25	25	43	43	86

Table 1. Summary of 4 individuals' visual pigments in the dusky flathead *P. fuscus*, measured using microspectrophotometry. Wavelength of maximum absorbance (λ_{max}) values are given ± one standard deviation.

	Rod	Single cones	Twin cones		
			Higher	Lower	All
λ_{max} of mean prebleach spectrum (nm)	508.9	461.8	525.8	526.9	524.4
Mean prebleach λ_{max} (nm)	508.7 ±9.5	461.6 ±1.4	526.2 ±4.3	527.4 ±4.2	525.1 ±4.2
Number of cells	44	17	83	40	43
$\underline{\lambda}_{max}$ of mean difference spectrum (nm)	516.3	463.1	526.2	525.5	526.9
Absorbance change at λ_{max} of difference spectrum	0.019	0.046	0.053	0.051	0.056
Mean difference spectrum λ_{max} (nm)	512 ±6.5	463 ±2.4	526.6 ±4.0	527.5 ±3.8	525.4 ±4.1
Number of cells	13	12	76	37	35

Table 2. Summary of 3 individuals' visual pigments in the blue-spotted flathead *P. caeruleopunctatus* measured using microspectrophotometry. Wavelength of maximum absorbance (λ_{max}) values are given ± one standard deviation.

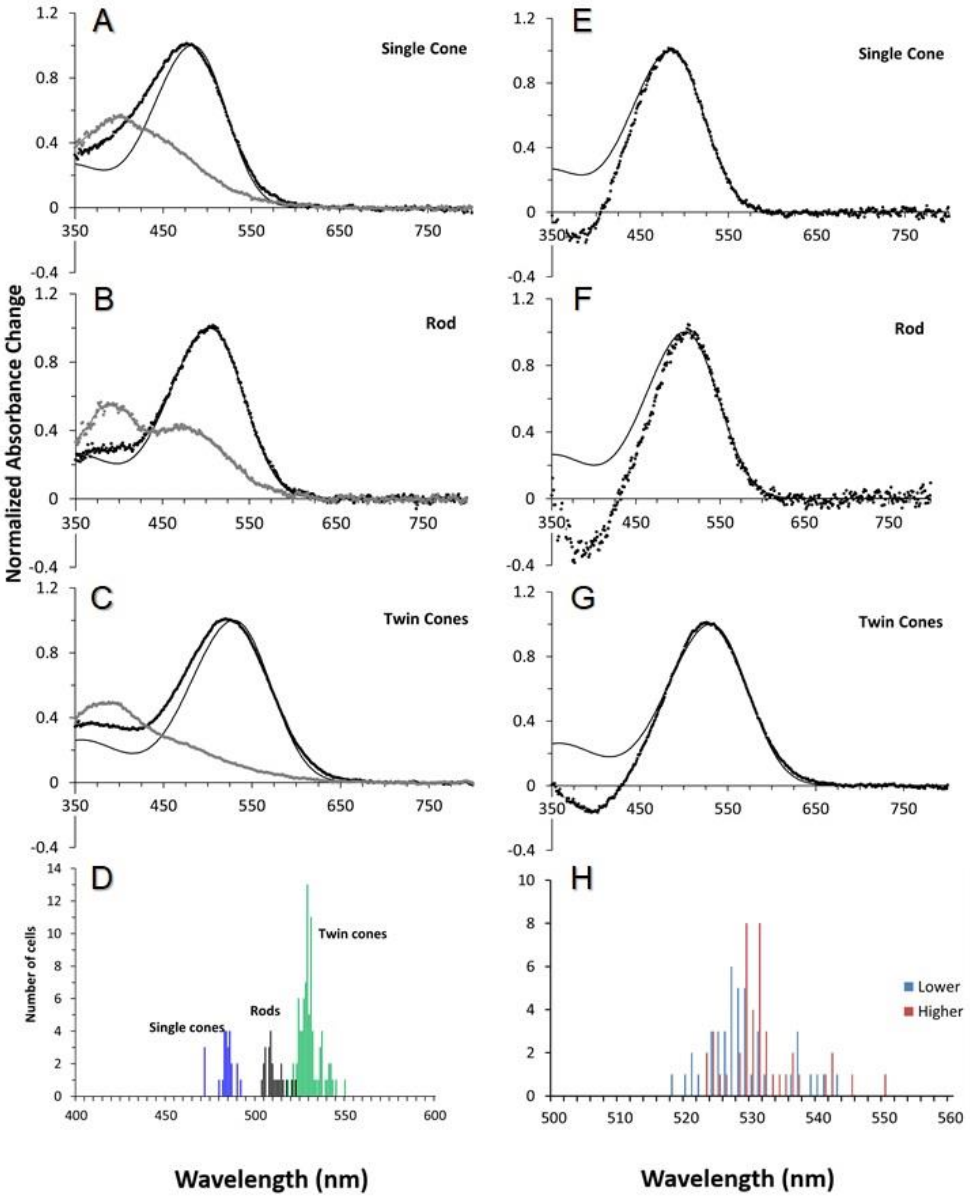

Figure 4. MSP analysis of dusky flathead *P. fuscus*. (A-C) Normalised pre-bleach (black circles) and post-bleach (grey circles) absorbance spectra of visual pigments. Pre-bleach spectra are overlayed with a best-fitted rhodopsin templates (bold line; Govardovskii et al., 2000). Post-bleach spectra are fitted with a variable point running average (thin line). (D) The spectral distribution of the wavelengths of maximum absorbance (λ_{max}) of the individual cone visual pigment difference spectra used to create the mean spectra. The group labelled as Twin cones in the histogram includes both members of the twin cone pair. (E-G) Normalized mean difference spectra (black circles) and best-fitted rhodopsin visual pigment templates (lines) for the visual pigments. Difference spectra represent the change in absorbance of the outer segment on bleaching with white light (see text for details). (H) The spectral distribution of the wavelengths of maximum absorbance (λ_{max}) of the higher and lower twin cones of the twin cone pair visual pigment difference spectra used to create the twin cone mean spectra.

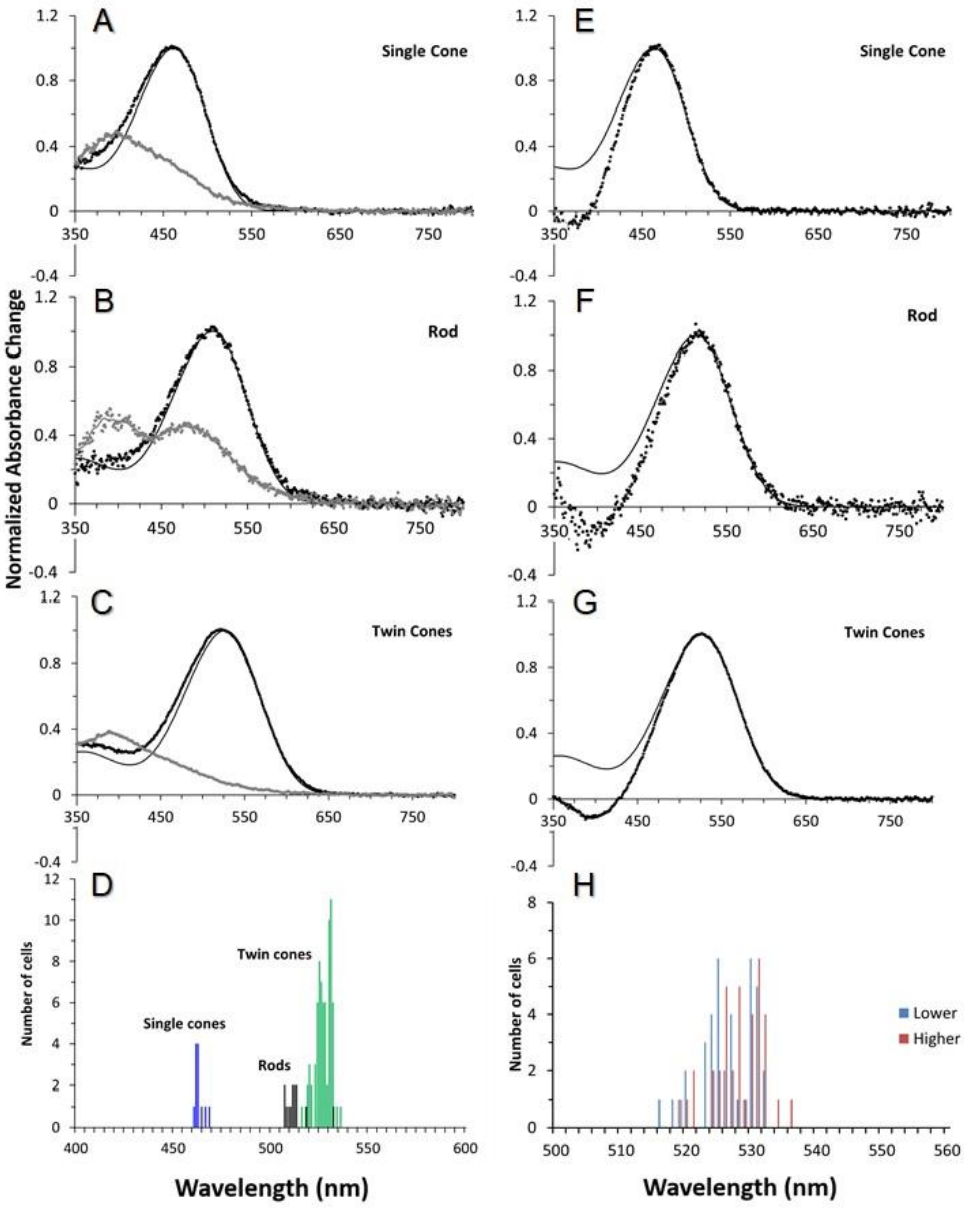

Figure 5. MSP analysis of blue-spotted flathead *P. caeruleopunctatus*. (A-C) Normalised pre-bleach (black circles) and post-bleach (grey circles) absorbance spectra of visual pigments. Pre-bleach spectra are overlayed with a best-fitted rhodopsin templates (bold line; Govardovskii et al., 2000). Post-bleach spectra are fitted with a variable point running average (thin line). (D) The spectral distribution of the wavelengths of maximum absorbance (λ_{max}) of the individual cone visual pigment difference spectra used to create the mean spectra. The group labelled as Twin cones in the histogram includes both members of the twin cone pair. (E-G) Normalized mean difference spectra (black circles) and best-fitted rhodopsin visual pigment templates (lines) for the visual pigments. Difference spectra represent the change in absorbance of the outer segment on bleaching with white light (see text for details). (H) The spectral distribution of the wavelengths of maximum absorbance (λ_{max}) of the higher and lower twin cones of the twin cone pair visual pigment difference spectra used to create the twin cone mean spectra.

Spectrophotometry of pre-retinal structures

The ocular media of both dusky and blue-spotted flathead have high transmittance from 800 nm until approximately 400 nm where transmittance decreases rapidly before it ceases entirely below approximately 390 nm (Figure 6.). The wavelength of 0.5 transmittance (λ_{T50}) was 412 nm in the dusky flathead and 405 nm in the blue-spotted flathead. Absorbance by the lens is the limiting factor for light transmittance in both the dusky and blue-spotted flathead. No noticeable effect on transmittance due to the corneal iridescence observed in blue-spotted flathead was recorded, but corneal iridescence may change after death. The effects those changes have on ocular transmittance is as yet not quantified.

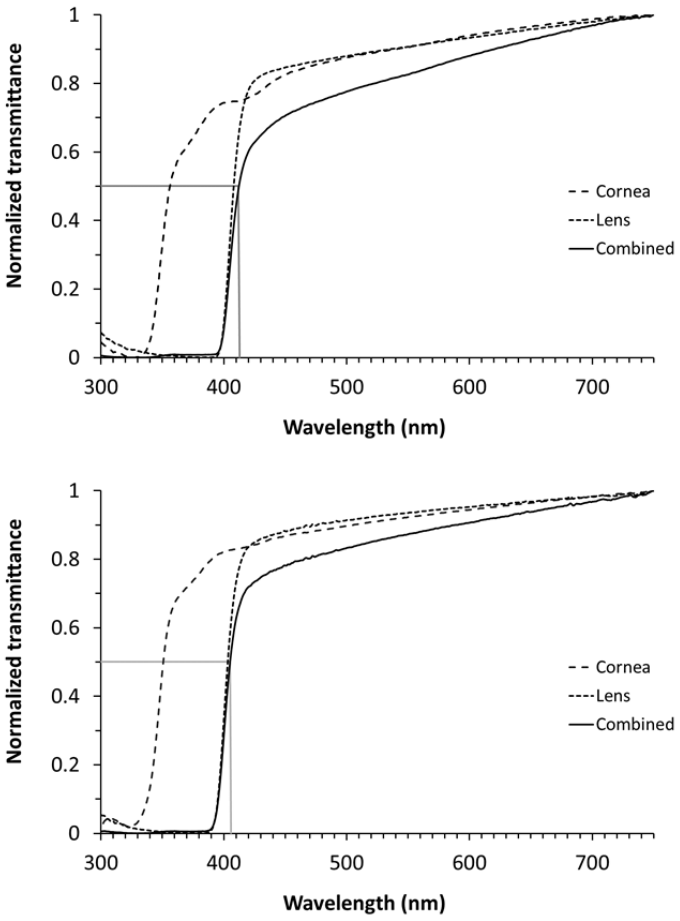

Figure 6. Transmittance of the individual components and combined ocular media of dusky flathead *P. fuscus* (top) and blue-spotted flathead *P. caeruleopunctatus* (bottom). Mean measurements of the intact cornea and lens to give the transmittance along the optic axis of the combined pre-retinal ocular media (combined). The wavelength of 0.5 transmittance λT0.5 of dusky flathead was 412 nm and blue-spotted flathead λT0.5 was 405 nm.

Isodensity mapping of ganglion cells

Topographic contour maps shown in Figure 7. summarise the ganglion cell distribution in the dusky flathead and blue-spotted flathead retina. The dusky flathead (Figure 7.), topographic map shows an elongated area of high density with a gradient between 12,000 and 20,000 cells mm² (peak density 29500 cells per mm²) located in the dorsal retina. The lowest density region lies in the ventral retina with densities less than 2000 cells mm² close to the falciform process. The blue-spotted flathead (Figure 7.), topographic map shows a similar density topography with an elongated area of high density with a gradient between 12,000 and 20,000 cells mm² (peak density 27200 cells per mm²) located in the dorsal retina. The lowest density regions in the blue-spotted flathead also occurs in the ventral retina with less than 2000 cells mm². Estimates of spatial resolution using peak ganglion cell density in the elongated area were similar between species but highest in blue-spotted flathead with a value of 9.86 cycles per degree, the recorded value for dusky flathead was 8.09 cycles per degree.

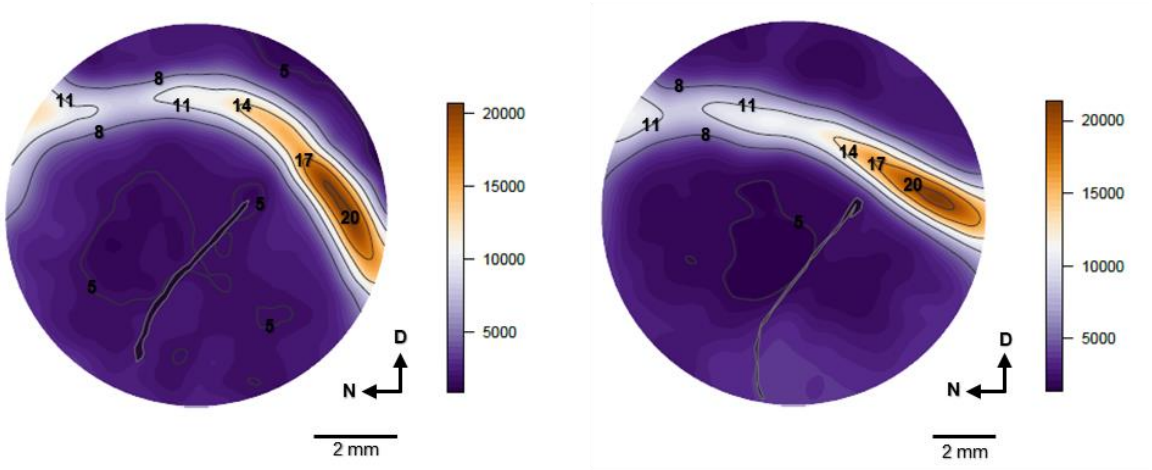

Figure 7. Isodensity contour maps show the topography of the neural cell distribution in dusky flathead *P. fuscus* (Left) and blue-spotted flathead *P. caeruleopunctatus* (Right). Scale bar (right of map) indicates cell density per mm². Arrows indicate retinal orientation; Dorsal (D) and Nasal (N). The falciform process and optic nerve head positions are indicated by the dark area. Contour numbers represent cell density per mm² $\times 10^3$.

Discussion

In this study, we examined the peripheral visual system of two benthic teleost species from the same family in order to identify possible variations in visual ecology that may reflect adaptations to differing depth profiles and other habitat characteristics. We measured the number and spectral absorbance properties of the retinal photoreceptor (rod and cone) visual pigments, the spectral transmittance of the ocular media, and the topographic distribution of neurons in the ganglion cell layer. Both species displayed a similar topographic distribution of ganglion cells with a dorsally located extended area of high cell density. Variability between the species was observed in general structural morphology but most significantly in the recorded single cone visual pigments, blue-spotted flathead possessing a more blue-shifted single cone visual pigment (mean λ_{max} 461) than the single cone visual pigment recorded in dusky flathead (mean λ_{max} of 483 nm).

Microspectrophotometry data

The array and spectral absorbance characteristics of visual pigments in both blue-spotted flathead *P. caeruleopuntatus* and dusky flathead *P. fuscus* are different than that found in other similar classed flatfish of similar regions (*Pleuronectes platessa*, Loew & Lythgoe, 1978; *Platichthys stellatus,* Iwanicki, 2016). Both of the observed flathead species have a less diverse array of visual pigments than that found in their other flatfish counterparts, some of which possess upwards of seven visual pigments, identified in part to genetic opsin identification (*Platichthys stellatus,* Iwanicki, 2016). The broad wavelength observed in the visual pigments found in both flathead species and the presence of 'rare' cones suggests the possibility of other visual pigments in both species, all of which could be investigated further with genetic opsin identification testing. Initial observations made in this study suggest that both species have the potential for dichromatic colour vision. The rod visual pigments of both blue-spotted (mean λ_{max} 508) and dusky flathead (mean λ_{max} 504) fall within the normal range of observed rod λ_{max} for marine teleosts (Loew & Lythgoe, 1978).

The most significant variation between the visual pigments of both species was in the single cones. The wavelength of maximum mean absorption spectra of single cone visual pigment in blue-spotted flathead was shorter (mean λ_{max} 461) compared to dusky flathead (mean λ_{max} 483). Visual pigments in teleost species are often correlated with the environmental conditions (Lythgoe *et al.*, 1994) and those found in deeper waters often possess more blue

shifted visual pigments (Lythgoe & Partridge, 1989). It seems likely, therefore, that the difference in single cone pigments between blue-spotted and dusky flathead reflects the difference in their habitat depth ranges, blue-spotted flathead (25-100m) and dusky flathead (1-25m) (Bray, 2017). The blue-shift in the single cone visual pigment of blue-spotted flathead would better match available light in both open and deeper oceanic regions (Lythgoe, 1968; Partridge *et al.*, 1989), this would allow it to hunt better across the oceanic floor. In contrast, the long-wavelength–shifted single cone pigment found in the dusky flathead would help it contend more with the greater proportion of green light present in shallower coastal and estuarine regions due to the higher levels of organic matter (Jerlov, 1968; Lythgoe, 1968).

During the microspectrophotometric experiments, a few rare single cones with λ_{max} values at shorter wavelengths (~450 nm) were observed in dusky flathead specimens; while these have not been presented in the present analysis, this will be investigated in future. These sparse blue cones could be a distinct cone class present in adults. However, ontogenetic shifts in visual pigments expression are known to occur in teleost species during development and changes in habitat (Shand *et al.*, 2002). The recorded visual pigments may be a remnant from early developmental stages, and further study of visual pigment development during dusky flathead life stages would be needed to determine this.

Twin cone visual pigments were very similar between both species, with an almost identical λ_{max} value in both the dusky flathead (mean λ_{max} 528 nm) and the blue-spotted flathead (mean λ_{max} 526 nm). This is in contrast to the apparent difference in λ_{max} of the single cones between the two species. Interestingly, the most reliable correlation between habitat light and visual pigment spectral tuning in fishes is seen for the twin cones pigments, rather than the single cones (Lythgoe *et al.*, 1994). In the case of the flathead it is not immediately obvious therefore what is driving the spectral tuning of the twin cone pigments and further work is required to understand how these species use their eyes and under what environmental conditions. The ambush-style feeding behaviour observed in flathead species (Barnes *et al.*, 2011; McComb *et al.*, 2013; Gray & Barnes, 2015) would likely require visual pigments that are tuned to detect dark silhouettes against a light background, a visual task that is optimised by visual pigments matched to the down-welling light; in this case we would predict a difference in twin cone pigment λ_{max} between the dusky and blue-spotted flatheads. However, the fact that this was not observed indicates that other selection pressures may drive visual pigment tuning, such as colour discrimination.

The distribution of both species continually shifts across both depth and distance to shore, because of this we had expected to see a short wavelength shift in one of the twin cones, similar to that observed in other closely related species that share similar niche segregation (Lythgoe *et al.*, 1994). Two prevalent hypotheses in fish visual ecology regarding the spectral tuning of pigments (Lythgoe, 1968; Lythgoe & Partridge, 1989), the 'sensitivity' hypothesis and the 'contrast' hypothesis. The sensitivity hypothesis lends belief that a fish would tend to possess if any, visual pigments best suited to capture the most available light available in its given environment. Whereas, visual pigments in fish, under the contrast hypothesis would benefit the animal most if tuned to increase their ability to contrast objects (food) from the background (environment). It could be that the twin cones are matched to the most common wavelengths of available light and are of a matched pigment for enhanced sensitivity under most conditions (dark object against a light background), whereas the single cone pigment might be offset for improved contrast under certain visual conditions (bright object against a dark background).

Analysis of the data obtained from the two different members of the twin cone pair (i.e. the higher and lower λ_{max} member in each individual pair) showed a clear overlap in the λ_{max} values of the pigments present. This suggests that the twin cones of the flathead in these two species are identical twins in terms of their spectral sensitivity.

In some recorded spectra for individual twin cone outer segments, there was a small amount of deviation between the measured absorbance data and the fitted template between about 70% and 100% of normalized absorbance on the short wavelength limb, which may indicate that more than one opsin (or a mixture of chromophores) might be present in the outer segment. The twin cone visual pigments in both of these species were similar to those found in other species (Wang *et al.*, 2009) and based on this and other publications we would predict the presence of Rh1 (rod), SWS 2 (single cone), and either RH2 or M/LWS opsins (twin cones) in the studied flathead species. Analysis of the genome or the retinal transcriptome would have to be conducted to determine which opsins are present in the flathead and the possibility of opsin co-expression in the twin cones.

Spectral properties of the ocular media

The spectral absorbance of the ocular media was similar between both species. This is perhaps unsurprising as high transmittance of light to the retina is essential, especially in the turbid and/or deep-water environments these flathead species typically inhabit. The lack of any

substantial transmittance below 390 nm makes the presence of UV visual pigments in these species unlikely.

The observed corneal iridescence in blue-spotted flathead appeared not to alter the spectral transmittance of the species compared to that observed in dusky flatheads. Corneal iridescence is known to degrade post-mortem (Shand & Lythgoe, 1987), but the effects of this are not yet quantified. Transmittance readings were taken in air and this may have altered the recorded transmittance of the ocular media, particularly that of the cornea and may have contributed to iridescence degradation. Further observations of the intact eye and the isolated ocular media will be required to elucidate the function of corneal iridescence on spectral transmission in blue-spotted flathead. Corneal iridescence in blue-spotted flathead may provide similar function to that observed in other flatfish (*Pleuronectes platessa*, Shand and Lythgoe, 1987), by changing with exposure to shorter or longer wavelengths of light it may reduce harmful exposure to light when moving from deep to shallow environments.

Topographic distribution of retinal neurons

Topographical mapping of neuronal cell density in the ganglion cell layer across the retina of both dusky and blue-spotted flathead showed a similar distributional pattern to other benthic flatfish species, including the European hake (*Merluccius merluccius*) (Bozzano & Catalán, 2002). The highest density of ganglion cells was located in an elongated area in the dorsal retina, with a decreasing gradient in cell density in a horizontal streak-like pattern along the dorsal retina. The lowest cell density for both dusky and blue-spotted was in the ventral retina, closely associated with the falciform process.

The topographical distribution of ganglion cells indicates a central region of visual resolution directed at a downward angle towards the mouth region, possibly to aid in feeding and prey capture. Ganglion cell functionality may not be accurately represented by the topographic maps as ganglion cell morphology was not assessed during this study. The determination of the distribution of ganglion cells associated with motion detection and ganglion cells associated with high resolution vision would require further morphological and physiological analysis.

Spatial resolution of high density regions, calculated from peak cell density counts showed that both species had similar spatial resolution power, but it was slightly higher in blue-spotted flathead, with a spatial resolution value of 9.86 cycles per degree, compared to 8.09 cycles per

degree in the dusky flathead. The difference in spatial resolution power may be attributed to the fact that only a single retina of each species was available for counting.

Visual ecology

Study of the visual capabilities of both flathead species revealed that both species possess very similar visual systems, both species possessing rods, one spectral type of single cone and identical twin cones. Adaptations in the spectral sensitivity characteristics of both species are believed to be associated with the environmental light conditions of their known ranges.

Spatial resolution and topographic distribution of ganglion cells observed in the sampled retina of both species were very similar. Spatial resolution in blue-spotted flathead retina studied was higher in cycles per degree than that of the dusky flathead; this may be a result of the difference in depth range or a slight difference in dietary composition often observed in flathead species (Barnes *et al.*, 2011; Coulson *et al.*, 2015). Blue-spotted flathead may feed more on crustacea and therefore require finer spatial resolution than dusky which are known to feed predominantly on smaller teleosts.

Flathead are often caught as by-catch in trawler nets and are observed to not visibly react to approaching trawl bars (Bublitz, 1996). Based on our calculated spatial resolution and potential sensitivity to motion both dusky and blue-spotted flathead would be able to perceive approaching trawler bars. A lack of avoidance towards trawler bars may purely be behavioural.

During the study, morphological variations between the species was also noted, for example in the observed blue-spotted flathead the overall eye size relative to body length, the vastly increased size of the choroid gland and the presence, and strength of corneal iridescence was greater than that found in any observed dusky specimens. Blue-spotted flathead were also noted to possess a stratum argenteum.

Conclusion

Study of the visual adaptions in closely related teleost species (Lythgoe *et al.*, 1994) has provided important insights into ecological- and environmental-niche-driven variability in visual systems. This study has revealed similar adaptations in the visual systems of flathead that are congruent with other teleost species with similar differences in habitat and depth range. The study of other related species, including the southern sand flathead (*Platycephalus bassensis*), tiger flathead (*Platycephalus richardsoni*) and northern sand flathead (*Platycephalus endrachtensis*) (Bray, 2017), would provide additional information necessary to identify the ecological and environmental pressures driving these adaptations in flathead visual systems and those of other predatory benthic fishes in general.

References

Abràmoff, M. D., Magalhães, P. J. and Ram, S. J. (2004) ‘Image processing with ImageJ’, *Biophotonics international*. Laurin Publishing, 11(7), pp. 36–42.

Amezcua, F. and Nash, R. D. M. (2001) ‘Distribution of the order Pleuronectiformes in relation to the sediment type in the North Irish Sea’, *Journal of Sea Research*, 45(3–4), pp. 293–301. doi: 10.1016/S1385-1101(01)00044-2.

Barnes, L. M., Leclerc, M., Gray, C. A. and Williamson, J. E. (2011) ‘Dietary niche differentiation of five sympatric species of Platycephalidae’, *Environmental Biology of Fishes*, 90, pp. 429–441.

Barnes, L. M., Gray, C. A. and Williamson, J. E. (2011) ‘Divergence of the growth characteristics and longevity of coexisting Platycephalidae (Pisces)’, *Marine and Freshwater Research*, 62(11), pp. 1308–1317. doi: 10.1071/MF11045.

Bozzano, A. and Catalán, I. (2002) ‘Ontogenetic changes in the retinal topography of the European hake, Merlucciusmerluccius: implications for feeding and depth distribution’, *Marine Biology*. Springer, 141(3), pp. 549–559.

Bray,D.J.(2017) *Platycephalus,Fishes of Australia*. Available at: http://fishesofaustralia.net.au/home/genus/1177 (Accessed: 20 January 2018).

Bublitz, C. G. (1996) ‘Quantitative evaluation of flatfish behavior during capture by trawl gear’, *Fisheries Research*, 25(3–4), pp. 293–304. doi: 10.1016/0165-7836(95)00431-9.

Cohn, B. A., Collin, S. P., Wainwright, P. C. and Schmitz, L. (2015) ‘Retinal topography maps in R: New tools for the analysis and visualization of spatial retinal data’, *Journal of vision*. The Association for Research in Vision and Ophthalmology, 15(9), p. 19.

Coimbra, J. P., Nagloo, N., Hart, N. S, and Collin, S P. (2009) ‘Number and distribution of neurons in the retinal ganglion cell layer in relation to foraging behaviors of tyrant flycatchers’, *Journal of Comparative Neurology*. Wiley-Blackwell, 514(1), pp. 66–73. doi: 10.1002/cne.21992.

Collin, S. P. and Pettigrew, J. D. (1988a) ‘Retinal topography in reef teleosts. II. Some

species with prominent horizontal streaks and high-density areae.', *Brain, behavior and evolution.* [Basel, Switzerland] :, pp. 283–295. doi: 10.1159/000116595.

Collin, S. P. and Pettigrew, J. D. (1988b) 'Retinal topography in reef teleosts I: Some species with well-developed areae but poorly developed streaks.', *Brain, behavior and evolution*, 31(5), pp. 269–282.

Collin, S. P. and Pettigrew, J. D. (1989) 'Quantitative comparison of the limits on visual spatial resolution set by the ganglion cell layer in twelve species of reef teleosts.', *Brain, behavior and evolution*, 34, pp. 184–192. doi: 10.1159/000116504.

Coulson, P. G., Platell, M., Clarke, K. R. and Potter, I C. (2015) 'Dietary variations within a family of ambush predators (Platycephalidae) occupying different habitats and environments in the same geographical region', *Journal of Fish Biology*, 86, pp. 1046–1077.

Douglas, W. A. and Lanzing, W. J. R. (1981) 'Colour change and visual cues in sand flathead, Platycephalus arenarius (Ramsay and Ogilby)', *Journal of Fish Biology*, 18, pp. 619–628.

Duffy-Anderson, J. T., Blood, D. M., Cheng, W., Ciannelli, L., Matarese, A. C., Sohn, D., Vance, T. C. and Vestfals, C. (2013) 'Combining field observations and modelling approaches to examine Greenland halibut (Rienhardtius hippoglossoides) early life ecology in the southern Bering Sea', *Journal of Sea Research*, 75, pp. 96–109.

Froese, R. and Pauly, D. (2010) 'FishBase'. Fisheries Centre, University of British Columbia.

Garza-Gisholt, E., Kempster, R. M., Hart, N. S. and Collin, S. P. (2015) 'Visual Specializations in Five Sympatric Species of Stingrays from the Family Dasyatidae', *Brain, behavior and evolution*. Karger Publishers, 85(4), pp. 217–232.

Geffen, A. J., van der Veer, H. W. and Nash, R. D. M. (2007) 'The cost of metamorphosis in flatfishes', *Journal of Sea Research*, 58(1), pp. 35–45. doi: 10.1016/j.seares.2007.02.004.

Govardovskii, V. I., Fyhrquist, N., Reuter, T., Kuzmin, D. G. and Donner, K. (2000) 'In search of the visual pigment template', *Visual Neuroscience*. Macquarie University, 17(4), pp. 509–528. doi: 10.1017/S0952523800174036.

Gray, C. A. and Barnes, L. M. (2008) *Reproduction and growth of dusky flathead (Platycephalus fuscus) in NSW estuaries*. NSW Department of Primary Industries. Available at: http://www.fish.gov.au/reports/Documents/Gray_and_Barnes_2008_Dusky_Flathead_Final_Report_REPORT.pdf.

Gray, C. A. and Barnes, L. M. (2015) 'Spawning, maturity, growth and movement of Platycephalus fuscus (Cuvier, 1829) (Platycephalidae): fishery management considerations', *Journal of Applied Ichthyology*, 21, pp. 442–450. Available at: http://onlinelibrary.wiley.com.simsrad.net.ocs.mq.edu.au/doi/10.1111/jai.12703/epdf.

Hart, N. S. (2002) 'Vision in the peafowl (Aves: Pavo cristatus)', *Journal of Experimental Biology*. The Company of Biologists Ltd, 205(24), pp. 3925–3935.

Hart, N. S. (2004) 'Microspectrophotometry of visual pigments and oil droplets in a marine bird, the wedge-tailed shearwater Puffinus pacificus: topographic variations in photoreceptor spectral characteristics', *Journal of Experimental Biology*, 207(7), pp. 1229–1240. doi: 10.1242/jeb.00857.

Hart, N. S., Theiss, S., Harahush, B. K. and Collin, S. P. (2011) 'Microspectrophotometric evidence for cone monochromacy in sharks', *Naturwissenschaften*, 98(3), pp. 193–201. doi: 10.1007/s00114-010-0758-8.

Hart, N. S., Partridge, J. C. and Cuthill, I. C. (1998) 'Visual pigments, oil droplets and cone photoreceptor distribution in the european starling (Sturnus vulgaris)', *Journal of experimental biology*, 201 (Pt 9)(April 2016), pp. 1433–1446. Available at: http://www.ncbi.nlm.nih.gov/pubmed/9547323.

Hoke, K., Evans, B. and Fernald, R. (2006) 'Remodeling of the cone photoreceptor mosaic during metamorphosis of flounder (Pseudopleuronectes americanus)', *Brain, Behavior and Evolution*, 68(4), pp. 241–254. doi: 10.1159/000094705.

Hopper, A. G. (2013) *Deep-water fisheries of the North Atlantic Oceanic slope*. Volume 296. Springer Science & Business Media.

Hughes, A. (1977) 'The Topography of Vision in Mammals of Contrasting Life Style: Comparative Optics and Retinal Organisation BT - The Visual System in Vertebrates', in

Crescitelli, F. et al. (eds) *The Visual System in Vertebrates*. Berlin, Heidelberg: Springer Berlin Heidelberg, pp. 613–756. doi: 10.1007/978-3-642-66468-7_11.

Hunt, D. E., Rawlinson, N. J. F., Thomas, G. A. and Cobcroft, J. M. (2015) 'Investigating photoreceptor densities, potential visual acuity, and cone mosaics of shallow water, temperate fish species', *Vision research*. Elsevier, 111, pp. 13–21.

Iwanicki, T. (2016) 'The visual opsins of the starry flounder (Platichthys stellatus), a new model for studying the physiological and molecular basis of fish vision and light sensitivity.' *Unpublished Masters Thesis, University of Victoria, Australia.*

Jerlov, N. G. (1968) *Optical Oceanography*. London: Elsevier.

Land, M. F. and Nilsson, D.-E. (2012) *Animal eyes*. Oxford University Press.

Levine, J. S. and MacNichol, E. F. (1985) 'Microspectrophotometry of primate photoreceptors: Art, artefact and analysis.', in *The Visual System*. A. Fein an. Liss New York, pp. 73–87.

Litherland, L. and Collin, S. (2008) 'Comparative visual function in elasmobranchs: Spatial arrangement and ecological correlates of photoreceptor and ganglion cell distributions', *Visual Neuroscience*. 2008/07/01. Cambridge University Press, 25(4), pp. 549–561. doi: DOI: 10.1017/S0952523808080693.

Loew, E. and Lythgoe, J. (1978) 'The ecology of cone pigments in teleost fishes', *Vision Research*, 18(6), pp. 715–722. doi: 10.1016/0042-6989(78)90150-5.

Lythgoe, J. (1968) 'Visual pigments and visual range underwater', *Vision Research*, 8(8), pp. 997–1012. doi: 10.1016/0042-6989(68)90073-4.

Lythgoe, J. N., Muntz, W. R. A., Partridge, J. C., Shand, J. and Williams, D. Mc B. (1994) 'The ecology of the visual pigments of snappers (Lutjanidae) on the Great Barrier Reef', *Journal of Comparative Physiology A*. doi: 10.1007/BF00191712.

Lythgoe, J. N. and Partridge, J. C. (1989) 'Visual pigments and the acquisition of visual information', *Journal of Experimental Biology*, 146(1), pp. 1–20. Available at: http://jeb.biologists.org/content/146/1/1.1.abstract.

MacNichol, E. F. (1986) ‘A unifying presentation of photopigment spectra’, *Vision Research*, 26(9), pp. 1543–1556. doi: https://doi.org/10.1016/0042-6989(86)90174-4.

Marshall, J. (2017) ‘Vision and lack of vision in the ocean’, *Current Biology*. Elsevier, 27(11), pp. 494–502. doi: 10.1016/j.cub.2017.03.012.

Marshall, J., Carleton, K. L. and Cronin, T. (2015) ‘Colour vision in marine organisms’, *Current Opinion in Neurobiology*, pp. 86–94. doi: 10.1016/j.conb.2015.02.002.

Marshall, N. J., Jennings, K., McFarland, W. N., Loew, E. R. and Losey, G. S. (2003) ‘Visual biology of Hawaiian coral reef fishes. III. Environmental light and an integrated approach to the ecology of reef fish vision.’, in *Copeia 3*, p. 467–480.

Matthiessen, L. (1880) ‘Untersuchungen über den aplanatismus und die periscopie der krystalllinsen in den augen der fische’, *Archiv für die gesamte Physiologie des Menschen und der Tiere*. Springer, 21(1), pp. 287–307.

McComb, M., Kajiura, S., Horodysky, A. and Frank, T. (2013) ‘Comparative Visual Function in Predatory Fishes from the Indian River Lagoon’, *Physiological and Biochemical Zoology*, 86(3), pp. 285–297. doi: 10.1086/670260.

McFarland, W. (1991) ‘Light in the sea: The optical world of elasmobranchs’, *Journal of Experimental Zoology Supplement*, 256(5), pp. 3–12. doi: 10.1002/jez.1402560503.

McFarland, W. N. and Loew, E. R. (1983) ‘Wave produced changes in underwater light and their relations to vision’, *Environmental Biology of Fishes*, 8(3–4), pp. 173–184. doi: 10.1007/BF00001083.

Nelson, J. S., Grande, T. C. and Wilson, M. V. H. (2016) *Fishes of the World*. John Wiley & Sons.

Ollivier, F. J., Samuelson, D. A., Brooks, D. E., Lewis, P. A., Kallberg, M. E. and Komáromy, A. M. (2004) ‘Comparative morphology of the tapetum lucidum (among selected species)’, *Veterinary ophthalmology*. Wiley Online Library, 7(1), pp. 11–22.

Partridge, J. C. *et al.* (1989) ‘Interspecific variation in the visual pigments of deep-sea fishes’, *Journal of Comparative Physiology A*. Springer, 164(4), pp. 513–529.

Partridge, J. C., Archer, S. N. and Lythgoe, J. N. (1988) ‘Visual pigments in the individual

rods of deep-sea fishes', *Journal of Comparative Physiology A*. Springer, 162(4), pp. 543–550.

Pauly, D. (1994) 'A framework for latitudinal comparisons of flatfish recruitment', *Netherlands Journal of Sea Research*, 32(2), pp. 107–118.

Pauly, D., Christensen, V., Dalsgaard, J., Froese, R. and Torres, F. Jr. (1998) 'Fishing down marine food webs', *Science*, 279(5352), pp. 860–863. Available at: http://www.sciencemag.org/content/279/5352/860.full.pdf (Accessed: 25 July 2014).

Savino, J. F. and Stein, R. A. (1989) 'Behavior of fish predators and their prey: habitat choice between open water and dense vegetation', *Environmental Biology of Fishes*. Springer, 24(4), pp. 287–293.

Schieber, N. L., Collin, S. P. and Hart, N. S. (2012) 'Comparative retinal anatomy in four species of elasmobranch', *Journal of Morphology*, 273(4), pp. 423–440. doi: 10.1002/jmor.11033.

Shand, J., Hart, N. S., Thomas, N. and Partridge, J. C. (2002) 'Developmental changes in the cone visual pigments of black bream Acanthopagrus butcheri.', *The Journal of experimental biology*, 205(Pt 23), pp. 3661–3667.

Shand, J. and Lythgoe, J. N. (1987) 'Light-induced changes in corneal iridescence in fish', *Vision Research*, 27(2), pp. 303–305. doi: https://doi.org/10.1016/0042-6989(87)90193-3.

Sohn, D. (2009) *Ecology of Greenland Halibut (Reinhardtius hippoglossoides) during the Early Life Stages in the Eastern Bering Sea and Aleutian Islands*. Oregon state university.

Sterratt, D. C., Lyngholm, D., Willshaw, D. J. and Thompson, I. D. (2013) 'Standard Anatomical and Visual Space for the Mouse Retina: Computational Reconstruction and Transformation of Flattened Retinae with the Retistruct Package', *PLOS Computational Biology*. Public Library of Science, 9(2), p. e1002921. Available at: https://doi.org/10.1371/journal.pcbi.1002921.

Theiss, S. M., Lisney, T. J., Collin, S. P. and Hart, N. S. (2007) 'Colour vision and visual ecology of the blue-spotted maskray, Dasyatis kuhlii Müller & Henle, 1814', *Journal of Comparative Physiology A*, 193(1), pp. 67–79. doi: 10.1007/s00359-006-0171-0.

Ullmann, J. F. P., Moore, B. A., Temple, S. E., Fernández-Juricic, E. and Collin, S. P. (2012) 'The Retinal Wholemount Technique: A Window to Understanding the Brain and Behaviour', *Brain, Behavior and Evolution*, 79(1), pp. 26–44. doi: 10.1159/000332802.

Walls, G. L. (1942) *The Vertebrate Eye and Its Adaptive Radiation*. Cranbrook Institute of Science. doi: 10.1097/00006324-194301000-00005.

Wang, F. Y., Yan, H. Y., Chen, J. S., Wang, T. Y. and Wang, D. (2009) 'Adaptation of visual spectra and opsin genes in seabreams', *Vision research*. Elsevier, 49(14), pp. 1860–1868.

Appendix I

Cresyl Violet staining protocol for marine vertebrates

Procedure modified by Dr Nathan Hart and Anthony Seward from Lisney 2004.

Step	Solution	Duration
1	Absolute Ethanol	2-4 mins
2	95% Ethanol	2-4 mins
3	70% Ethanol	2-4 mins
4	50% Ethanol	2-4 mins
5	30% Ethanol	2-4 mins
6	Distilled Water	2-4 mins
7	0.05% Cresyl Violet	5-10 mins then check under microscope ± further staining
8	Distilled Water	2-4 mins
9	30% Ethanol	2-4 mins
10	50% Ethanol	2-4 mins
11	70% Ethanol	2-4 mins
12	95% Ethanol	2-4 mins
13	Absolute Ethanol	2-4 mins
14	Xylene 1	5 mins
15	Xylene 2	5-15 mins
16	Entellan ® New	Drop over retina and seal with coverslip

Appendix II

Absorbance spectra of rare cones encountered during microspectrophotometry

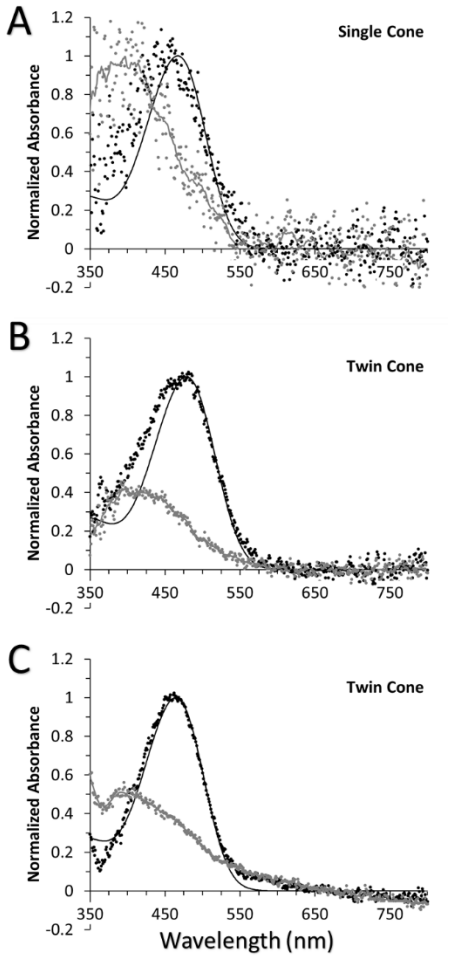

Legend: MSP analysis of rare photoreceptor outer segments in dusky flathead *P. fuscus* and blue-spotted flathead *P. caeruleopunctatus*. Normalised pre-bleach (black circles) and post-bleach (grey circles) absorbance spectra of visual pigments. Pre-bleach spectra are overlayed with a best-fitted rhodopsin templates (bold line; Govardovskii et al., 2000). Post-bleach spectra are fitted with a variable point running average (thin line). A. Single cone visual pigment of dusky flathead, n=1, approximate maximum absorbance (λ_{max}) 450 nm. B. Twin cone visual pigment of dusky flathead, n=2, approximate mean maximum absorbance (λ_{max}) 470 nm. C. Twin cone visual pigment of blue-spotted flathead, n=2, approximate mean maximum absorbance (λ_{max}) 460 nm.